Camera Placement Optimization Conditioned on Human Behavior and 3D Geometry

Pranav Mantini and Shishir K. Shah

Department of Computer Science,
University of Houston,
4800 Calhoun Road, Houston, Texas, USA
pmantini@cs.uh.edu, sshah@central.uh.edu

Keywords: Camera Placement Optimization, Human Motion Forecasting, Occupancy Map Estimation, Face Detection, Human Activity, Effective Surveillance

Abstract: This paper proposes an algorithm to optimize the placement of surveillance cameras in a 3D infrastructure. The key differentiating feature in the algorithm design is the incorporation of human behavior within the infrastructure for optimization. Infrastructures depending on their geometries may exhibit regions with dominant human activity. In the absence of observations, this paper presents a method to predict this human behavior and identify such regions to deploy an effective surveillance scenario. Domain knowledge regarding the infrastructure was used to predict the possible human motion trajectories in the infrastructure. These trajectories were used to identify areas with dominant human activity. Furthermore, a metric that quantifies the position and orientation of a camera based on the observable space, activity in the space, pose of objects of interest within the activity, and their image resolution in camera view was defined for optimization. This method was compared with the state-of-the-art algorithms and the results are shown with respect to amount of observable space, human activity, and face detection rate per camera in a configuration of cameras.

1 INTRODUCTION

Video surveillance is an integral part of many public areas such as airports, banks and train stations. The positioning and orientation of the cameras can play a significant role in enabling effective surveillance needs such as face detection, tracking, etc. The geographic distribution of cameras to enable effective surveillance can be scenario specific. For example, in a movie theater, it might be sufficient to deploy cameras at locations that exhibit dominant human activity, but at an airport, it may be imperative to deploy cameras to obtain a maximum visibility of observable space along with emphasis on areas with dominant human activity. Some common factors that should be taken into consideration while deploying cameras include visibility coverage and deployment costs.

Visibility coverage: In high security scenarios, the camera configuration should be optimized such that a maximal coverage of the observable space in the infrastructure can be obtained along with added emphasis on areas with dominant human activity. In low security scenarios, the camera configuration should at least guarantee the coverage of all the areas where dominant human activity would take place. The configuration can be made more effective by covering the most frequently used entry and exit points in the infrastructure. Furthermore, a camera configuration that maximizes the capture of specific pose of objects of interest (e.g., frontal image of the humans) with sufficient resolution is considered more effective.

Deployment cost: The configuration should guarantee the mentioned visibility coverage while deploying the least required number of cameras. Furthermore, having a minimal number of cameras has a significant impact on the available storage space with HD cameras becoming more prevalent and requiring higher storage space.

Designing a camera deployment configuration manually by taking into consideration the above factors can be extremely tedious and error prone. Automated camera network deployment optimization techniques are essential for a cost effective and safe environment. In this paper, we address the issue of obtaining effective surveillance by optimizing the deployment of cameras. In doing so, the multi-factorial issues of visibility coverage, deployment costs, preferred pose of objects of interest, and resolution are considered.

In this work, a camera configuration is considered to provide effective surveillance if the views across deployed cameras maximizes the following aspects while minimizing the total number of cameras.

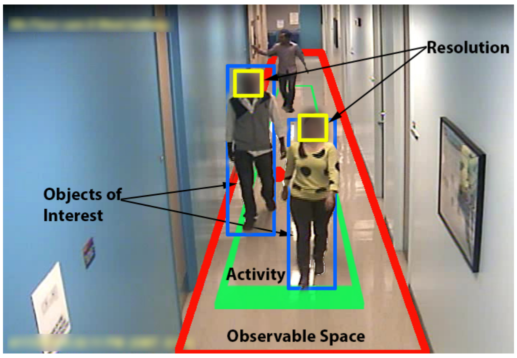

Figure 1: Example of an image from a single surveillance camera illustrating the four aspects of a camera view.

- the observable space,
- the view of regions within the infrastructure where dominant activity is expected,
- the ability to capture the preferred pose of objects of interest (e.g., frontal pose of humans), and
- their image resolution (e.g., face).

Consider a view from a single camera as shown in Figure 1. In the following, we discuss the four relevant aspects considered for an optimal camera configuration.

Maximize observable space in view: The information regarding the 3D geometry (floor) of the infrastructure can be used to maximize the observable space. In doing so, only the space that would be accessible by humans is considered relevant, as depicted by the red bounding box in Figure 1.

Maximize the view of regions with expected dominant human activity: Given the observable space, there are regions within it where one can expect dominant human activity to occur. This is illustrated by the green bounding box in Figure 1. All public infrastructures have entrances, exits and points of interest. Any doorway can be considered as an entrance or an exit. For simplicity they are referred to as nodes. In an infrastructure, different nodes are accessed with different frequencies. A node representing a common entrance or an exit has a high frequency of access as opposed to an employee's personal office. Given these nodes and their probabilities, human motion can be estimated or measured between the nodes to identify regions of high human activity.

Maximizes the ability to capture preferred pose of objects of interest: In this surveillance scenario, frontal pose of the humans can be considered to be the preferred pose as illustrated by the blue bounding boxes in Figure 1. The direction of motion of humans can be used to maximize the view of their frontal pose. Given the nodes, their probabilities, and trajectories followed by humans, this direction of motion can be identified.

Resolution of the imaged objects: The resolution of the face (yellow bounding box in Figure 1) could be considered as a feature of interest in the domain of human surveillance, and hence it's captured image resolution would be expected to be high. Similar to the previous step, the trajectories provide the direction of motion for the humans. A location of a face can be assumed based on the estimate of the average human height. The number of rendered pixels of the bounding box representing the face in the image from the camera can be used for maximizing this quantity.

In this paper, we provide a solution for optimal placement of cameras while considering the above factors. The main contributions of the paper are:

- We propose a method to incorporate predicted human behavior for camera placement optimization.
- We propose a method to estimate the human activity based on the 3D geometry of the infrastructure.
- We propose a method to identify and cluster regions of plausible high human activity.
- We propose a metric to assess the quality of a camera configuration based on observable space, amount of activity in the view, preferred pose of objects of interest, and their image resolution.

2 PREVIOUS WORK

Camera placement optimization is a crucial problem in computer vision and has been explored by many researchers. Most of the early work puts emphasis on image resolution and were based on a single camera focused on a static object. The problem was to find the best position for the camera that maximizes the quality of features on an object (Tarabanis et al., 1995; Fleishman et al., 1999). Later, (Chen and Davis, 2000) proposed a metric based on resolution and occlusion characteristics of the object that assessed the quality of multiple camera configurations. The configuration was optimized based on this metric such that minimum occlusion would occur while ensuring a certain resolution. (Mittal and Davis, 2004) suggested a probabilistic approach for visibility analysis that captured the observable space aspect and calculated the probability of visibility of an object from at least one camera in the configuration. Then a cost function was defined that mapped the sensor parameters to the probability and the cost function was minimized by simulated annealing.

(Erdem and Sclaroff, 2004) suggested a binary optimization approach for the camera placement problem that captured both the observable space and resolution aspect. The polygon representing the space is fragmented into an occupancy grid and the algorithm tries to minimize the cost of a camera configuration while maintaining some specified spatial resolution. (Hörster and Lienhart, 2006a; Hörster and Lienhart, 2006b; Hörster and Lienhart, 2006c) proposed a linear programming approach that determines the calibration for each camera in the network that maximizes the coverage of the observable space with a certain resolution. (Ram et al., 2006; Sivaram et al., 2009) proposed a performance metric that evaluates the probability of accomplishing a task as a function of set of camera configurations. This metric took into consideration the objects of interest in the scenario and was defined to realize only images obtained in a certain direction (frontal image of the person). (Bodor et al., 2007) proposed a method, where the goal is to maximize the aggregate observable space across multiple cameras. An objective function that quantifies the resolution of the image and the motion trajectories of the object in the scene is defined. A variant of hill climbing method was used to maximize this objective function.

(Murray et al., 2007) applied coverage optimization combined with visibility analysis to address this problem. For each camera location, the coverage was calculated using visibility analysis. Maximal covering location problem (MCLP) and backup coverage location problem (BCLP) were used to model the optimum camera combinations and locations. (Malik and Bajcsy, 2008) suggested a method for optimizing the placement of multiple stereo cameras for 3D reconstruction. An optimization framework was defined using an error based objective function that quantifies the stereo localization error along with resolution constraints. A genetic algorithm was used to generate a preliminary solution and later refined using gradient descent. (Kim and Murray, 2008) also employed BCLP to solve the camera coverage problem. They suggested an enhanced representation of the coverage area by representing it as a continuous variable in contrast to a commonly used discrete variable. (Yabuta and Kitazawa, 2008) and (Debaque et al., 2009) also employed a combination of MCLP and BCLP for solving the optimum camera coverage problem. The former took into consideration the 3D geometry of the environment and supplemented the MCLP/BCLP problem by including a minimal localization error variable for both monoscopic and stereoscopic cameras. The optimization problem was solved using simulated annealing. In the latter, the MCLP/BCLP problem was supplemented using visibility analysis for optimization. (Huang et al., 2014) proposed a 2 stage approximation algorithm, the first part proposes a solution for the minimum watchmen tour problem and placed cameras along the estimated tour, the second part finds the solution to art gallery problem and added extra cameras to connect the guards. Most of the previous work emphasizes the importance of maximizing observable space and resolution of this space. There is little work addressing the significance of activity in the observable space along with obtaining useful data. This work address this by assumes equal importance to all four aspects which were ignored in the previous work.

Considering the 3D geometry of the environment is of significant value for the camera coverage optimization problem. In this paper, we focus on indoor scenarios and assume the availability of a complete 3D model of the environment where the camera network is to be deployed. To the best of our knowledge, this is the first work that takes into consideration the human activity in the scenario for designing an optimal camera network in the absence of any observations. Although (Bodor et al., 2007; Janoos et al., 2007) proposed the use of observed human activity for optimizing the camera placement, in the proposed work the human trajectories are simulated and not observed in order to identify regions with dominant human activity. Furthermore, (Ram et al., 2006; Sivaram et al., 2009) proposed the use of frontal view from observations as a task for optimizing the camera position unlike the proposed method that predicts frontal view based on human behavior. Finally, the human behavior in a given scenario is influenced by the 3D geometry of that environment (Mantini and Shah, 2014; Kitani et al., 2012). To the best of our knowledge, this is the first work that incorporates this information to optimize the camera network locations for video surveillance.

3 METHODOLOGY

3.1 Problem Formulation

Let G be the geometry (floors, ceilings, walls, etc.) of an infrastructure. Let $\{C_1, C_2, ..., C_\text{v}\}$ be a set of cameras located in G with configurations (like position, orientation, zoom, etc.) represented by $\{\omega_1, \omega_2, ..., \omega_\text{v}\}, \omega_i \in \Omega$, where Ω is the set of all possible configurations within G. Let $g : \omega \mapsto \mathbb{R}$ be an objective function. The problem is to find a set of optimal configurations $\{\omega_1^*, \omega_2^*, ..., \omega_\nu^*\}$ such that:

$$\{\omega_1^*, \omega_2^*, ..., \omega_\nu^*\} = \underset{\{\omega_1,\omega_2,...,\omega_\nu\}\in\Omega}{\arg\max} \sum_{i=1}^{\nu} g(\omega_i) \quad (1)$$

3.2 Camera Coverage Quality Metric

The function $g(.)$ quantifies the following aspects in view of the camera:

- amount of observable space,
- amount of view of regions with expected dominant activity,
- amount of ability to capture the preferred pose of objects, and
- image resolution of these objects.

(Janoos et al., 2007) proposed cell coverage quality metric to determine the coverage quality of a cell given a set of camera configurations by modeling realistic camera characteristics. A cell was defined as any unit of observable space, like a square in a grid or a triangle in a triangular mesh. Furthermore, they proposed a cost function that combines this metric with observed human occupancy for optimization. We extend this notion and define the Camera Coverage Quality Metric (CCQM) to quantify amount of observable space (A), amount view of regions with expected dominant activity (H), amount of ability to capture the preferred pose (F) and image resolution of these objects (R) for a camera configuration ω. The Camera Coverage Quality Metric ($CCQM$) is defined as:

$$CCQM(\omega) = g(A,H,F,R) = A(\omega) * H(\omega) * F(\omega) * R(\omega) \quad (2)$$

The optimal configuration of the cameras in G is defined as:

$$\{\omega_1^*, \omega_2^*, ..., \omega_\nu^*\} = \underset{\{\omega_1,\omega_2,...,\omega_\nu\}\in\Omega}{\arg\max} \sum_{i=1}^{\nu} CCQM(\omega_i) \quad (3)$$

Given ω, the functions $\{A,H,F,R\}$ are defined as follows. Without loss of generality we assume that the geometry to be viewed is represented by a triangular mesh containing triangles $\{t_1, t_2, ...t_n\}$ with centroids $\{c_1, c_2, ...c_n\}$. Let $\{t_1^\omega, t_2^\omega, ...t_m^\omega\}$ be the set of triangles in view of the camera with configuration ω.

Amount of observable space: The geometric area in view of the camera is used to quantify this aspect. The area of coverage function $A(\omega)$ is defined as:

$$A(\omega) = \frac{area\_in\_view}{total\_area} = \frac{\sum_{i=1}^{m} area(t_i^\omega)}{\sum_{i=1}^{n} area(t_i)} \quad (4)$$

Amount of view of regions with expected dominant activity: An occupancy map of a space quantifies how often a point is accessed compared to other points in that space. Let us assume an occupancy map as defined in (Mantini and Shah, 2014), that defines the frequency with which a triangle is accessed by humans. The same methodology as followed in (Mantini and Shah, 2014) is used to compute the occupancy map. The amount of occupancy is used to define the activity in the area. If $O(t)$ is the occupancy of the triangle t, then the human occupancy volume function is defined as:

$$H(\omega) = \frac{\sum_{i=1}^{m} O(t_i^\omega)}{\sum_{i=1}^{n} O(t_i)} \quad (5)$$

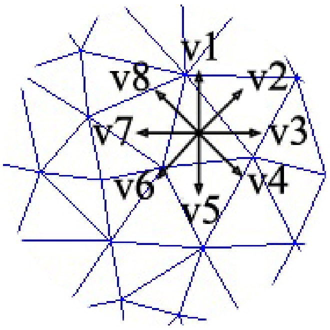

Figure 2: Vector discretization of triangle in a triangular mesh for creating a vector transition histogram from trajectories. .

Amount of ability to capture the preferred pose of objects: Humans are considered as objects of interest. Assuming that $\tau = \{T_1, T_2, ...\}$ be a set of trajectories followed by humans in the geometry G. These trajectories are used to quantify the amount of frontal view that can be obtained from the configuration ω. For every triangle t_i in the floor triangular mesh, direction discretization is performed and eight direction vectors $\{v_1^i, v_2^i, ..., v_8^i\}$ are defined as by (Zhou et al., 2010)(Figure 2).

In the following step, a vector transition histogram is constructed from the set of these trajectories. Consecutive points in the trajectory are considered to create a direction vector. If $T = \{p_1, p_2, ..., p_l\}$ is a trajectory of length l, for all set of consecutive points $\{p_{i-1}, p_i\}$, the direction vector is defined as $(p_i - p_{i-1})$. The bin corresponding to the triangle t in which the point p_{i-1} is located and the discretized direction vector subtending the smallest angle with $(p_i - p_{i-1})$ is incremented. Let $\Psi(t,v) \mapsto \mathbb{R}$ where $t \in \{t_1, t_2, ..., t_n\}$ and $v \in \{v_1, v_2, ..., v_8\}$ be the histogram function, then the frontal pose function $F(\omega)$

for a camera with center C is defined as:

$$
\begin{aligned}
F(\omega) = \frac{1}{m}\sum_{i=1}^{m}(((C-c_i)\cdot v_{k-1})\Psi(t_i,v_{k-1}) \\
+((C-c_i)\cdot v_k)\Psi(t_i,v_k) \\
+((C-c_i)\cdot v_{k+1})\Psi(t_i,v_{k+1}))
\end{aligned}
\tag{6}
$$

$$
k = \arg\max_{k}(v_k\cdot(C-c_i)) \tag{7}
$$

where t_i is the triangle with centroid c_i and v_k is the direction vector that subtends the smallest angle with $(C-c_i)$.

Image resolution of the object: This component of *CCQM* quantifies the resolution of the face. If the obtained image is far from the camera, the obtained resolution is very low and the image might not add any value to the system. This component is application dependent, it could be customized to obtain a sufficient resolution of any object, which could be just the face or the entire body of a human. We follow the methodology described by (Janoos et al., 2007) and define the function $R(\omega)$ for a camera with center C as:

$$
R(\omega) = \frac{1}{m}\sum_{i=1}^{m}\frac{\rho^{\omega}(t_i)}{\rho_{min}} \tag{8}
$$

$$
\begin{aligned}
\rho^{\omega}(t_i) = (2\pi * d(C,c_i)^2(1-\cos(\gamma/2)))^{-1} \\
(\sigma_{k-1}(C-c_i)\cdot v_{k-1} \\
+\sigma_k(C-c_i)\cdot v_k \\
+\sigma_{k+1}(C-c_i)\cdot v_{k+1})
\end{aligned}
\tag{9}
$$

where γ is the Y-field of view defined for the camera, $d(p_1,p_2)$ is the Euclidean distance between the points p_1 and p_2, k is as defined in Equation 7, σ is the number pixels the object occupies in the image and ρ_{min} is the user defined value that defines a minimum required resolution of an object in $pixels/inch$.

3.3 Optimization

Now that a metric is defined to assess the quality of a camera configuration ω, we perform a search in the geometry G to find the optimum parameter ω^*. Given the geometry and the domain knowledge, the search is performed to find two points, first on the ceiling to position the camera and the second on the floor to point the camera towards. Hence the parameter ω contains a pair of 3D points $\{v_1,v_2\}$. A variation of the hill climbing algorithm called the random-restart hill climbing (RRHC) algorithm is used for finding the optimum parameter ω^*. Random-restart hill climbing is an optimization search that provides near optimal performance (Zhang et al., 2014; Filho et al., 2010). The idea is to search a limited number of points randomly and choose the best start location for hill climbing optimization. Since the objective is to find two points, one on the floor and the second on the ceiling, this is done at two levels.

Algorithm 1 Optimal Pair

Require: v_1 (ceiling point), L (floor points list)
Ensure: v_2 (Optimal floor point)

```
procedure OPTIMAL–PAIR
    //Random Search
    $n \leftarrow$ number of points for random search
    $currentv_2 \leftarrow Random\_Solution(L)$
    $current \leftarrow CCQM(v_1, currentv_2)$
    for $(i = 1; i \leq n; i++)$ do
        $currentv_2 \leftarrow Random\_Solution(L)$
        $candidate \leftarrow CCQM(v_1, currentv_2)$
        if $candidate > current$ then
            $current \leftarrow candidate$
            $candidatev_2 \leftarrow currentv_2$
        end if
    end for
    //Hill Climbing
    $current \leftarrow CCQM(v_1, candidatev_2)$
    for $k \in neighbors(candidatev_2)$ do
        $currentv_2 \leftarrow candidatev_2.neighbor[k]$
        $candidate \leftarrow CCQM(v_1, currentv_2)$
        if $candidate > current$ then
            $current \leftarrow candidate$
            $v_2 \leftarrow currentv_2$
        end if
    end for
    $Return(v_2)$
end procedure
```

Optimal pair: This algorithm takes as input a point on the ceiling (v_1) along with the list of points on the floor as input and performs RRHC optimization to find the optimal pair v_2 (a point on the floor) for v_1 that maximizes CCQM (Algorithm 1).

RRHC optimization: This algorithm takes as input a list of points representing the ceiling (C) and another list representing the points on the floor (F) and performs RRHC to find the optimal parameters $\{v_1,v_2\}$ that maximizes CCQM for a camera, where v_1 is a point to position the camera and v_2 is a point for orienting the camera towards (Algorithm 2).

3.4 Framework

The framework for obtaining the optimal parameters $\{\omega_1^*,\omega_2^*,...,\omega_V^*\}$ given the geometry G is described in this section. The framework design is shown in Figure 3, which contains three modules.

1. **Model:** In this module, the infrastructure is modeled. This requires domain knowledge regard-

Algorithm 2 RRHC Optimization

```
Require: $C$ (ceiling points list), $F$ (floor points list)
Ensure: $v_1$, $v_2$ (Optimal pair)
procedure RRHC–OPTIMIZATION
    //Random Search
    $n \leftarrow$ number of points for random search
    $currentv_1 \leftarrow Random\text{–}Solution(C)$
    $currentv_2 \leftarrow Optimal\text{–}Pair(currentv_1)$
    $current \leftarrow CCQM(currentv_1, currentv_2)$
    for $(i = 1; i \leq n; i++)$ do
        $candv_1 \leftarrow Random\text{–}Solution(C)$
        $candv_2 \leftarrow Optimal\text{–}Pair(candv_1)$
        $candidate \leftarrow CCQM(candv_1, candv_2)$
        if $candidate > current$ then
            $Maxv_1 \leftarrow candv_1$
            $current \leftarrow candidate$
        end if
    end for
    //Hill Climbing
    $currentv_1 \leftarrow Maxv_1$
    $currentv_2 \leftarrow Optimal\text{–}Pair(currentv_1)$
    $current \leftarrow CCQM(currentv_1, currentv_2)$
    for $k \in neighbors(currentv_1)$ do
        $candv_1 \leftarrow currentv_1.neighbor(k)$
        $candv_2 \leftarrow Optimal\text{–}Pair(candv_1)$
        $candidate \leftarrow CCQM(candv_1, candv_2)$
        if $candidate > current$ then
            $current \leftarrow candidate$
            $v_1 \leftarrow candv_1$
            $v_2 \leftarrow candv_2$
        end if
    end for
    $Return(v_1, v_2)$
end procedure
```

ing the infrastructure such as entrances, exits and doors (nodes). Furthermore, knowledge regarding the frequency of accessing these nodes is also required. The output is a list of transitions between nodes.

2. **Data generation:** In this module, the data required for optimization is generated. The input is the list of node transitions from the previous module. First a list of trajectories are generated using CTF for each pair of nodes from the list. These are the list of trajectories described in section 3.2 for quantifying the amount of preferred pose of objects of interest. These trajectories are then given as input to a sub-module that accumulates the trajectories to create an occupancy map that describes the frequency with which humans access the geometry. This occupancy map is the function $O(t)$ described in section 3.2 for quantifying the amount of view of regions with dominant activity. Then the occupancy map is also input to a clustering algorithm to cluster points based on their occupancy and spacial location in the geometry.

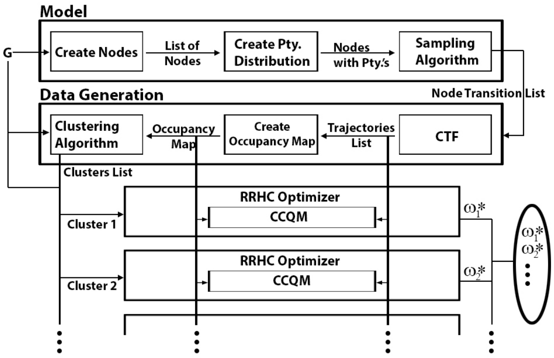

Figure 3: Framework with three modules, model, data generation, and RRHC optimizer for obtaining the optimal parameters $\{\omega_1^*, \omega_2^*, ..., \omega_v^*\}$.

3. **RRHC optimizer:** Each one of these clusters obtained is given as input to optimizers for finding the optimized configuration $\{\omega_1^*, \omega_2^*, ..., \omega_v^*\}$ for each cluster.

4 EXPERIMENTS

4.1 Implementation

4.1.1 Model

Given the geometry of an infrastructure, most humans follow trajectories with a goal of reaching a destination like an entrance, exit or a doorway. There is a certain probability associated with accessing these nodes based on the purpose they serve in the infrastructure. For example at an airport, passengers might access the ticket counter with a higher probability than a coffee shop or a restroom. The knowledge of this probability can be used to sample nodes that humans can transition between. Let us consider the following test case scenario. In Figure 4, the objective was to install a network of cameras that provide effective surveillance in the hallway.

Create nodes and probability distribution: The identified nodes are labeled with numbers in Figure 4. Let $\{n_1, n_2, ...\}$ be the nodes in the geometry G. In the absence of any observations of human motion, the probability of accessing a node was assumed to be proportional to the accommodation capacity of the

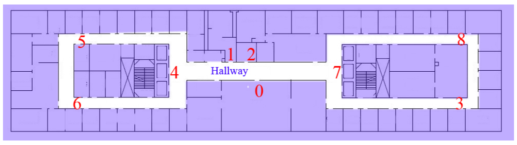

Figure 4: Floor plan of the test case scenario where the cameras are to be placed. The nodes are labeled with numbers.

room unless it was an entrance or exit. Implying that higher the capacity of a room to hold/seat people, the higher was the probability of accessing it. If $P_a(n_i)$ is a probability function that assigns probability to a node n_i and $A_c(n_i)$ is its accommodation capacity, then

$$P_a(n_i) \propto \begin{cases} 0 \text{ if } n_i = \text{entry/exit} \\ A_c(n_i) \text{ otherwise} \end{cases} \tag{10}$$

Sampling algorithm: The sampling algorithm was designed based on few assumption. A human entering the geometry G would eventually exit. A human would access a minimum of one node before exiting the geometry. Algorithm 3 describes the steps. In the example geometry in Figure 4, an entry $(4,7)$

Algorithm 3 Nodes Sampling

```
1: Choose a random entrance
2: Choose a node to access using $P_a$ as distribution
3: Choose randomly to either exit or access another node
4: if access another node then
5:     Choose another node excluding the current node
6:     Goto step 3
7: else
8:     Choose a random exit
9: end if
```

was chosen with equal probability, then a node was chosen that is not an exit based on the assigned probability (P_a). Now assuming that the human had transitioned to the node, the human could either choose to transition to another node or exit with equal probability. If the human chose to exit, the closest exit was chosen, else the human would choose to go to another node based on a calculated probability. The probability of choosing the second node changed because the node that the human was currently in was eliminated when calculating the probabilities. This gave a list of nodes $\{n_1^s, n_2^s, ...\}$ that can be used as start and end nodes for simulating trajectories.

4.1.2 Data Generation

Given the geometry of the environment along with the nodes and their assigned probabilities, the likely human motion in the infrastructure was simulated to identify regions of dominant human activity.

Contextual trajectory forecasting (CTF): CTF (Mantini and Shah, 2014) was used to simulate trajectories from the start node to the end node. Given the 3D geometry of the environment and the starting point and destination of a human, CTF is assembled on two assumptions. First, the human would follow a path that requires the shortest time to reach the destination, and second, the human would adhere to certain behavioral norms that are observed when walking in hallways. CTF uses a Markov model and assigns probabilities to points on the floor such that consecutive points are sampled from start to destination to form a trajectory that represents the shortest path while conforming to observed behavioral norms. CTF can take any pair of nodes $\{n_i^s, n_j^s\}$ from the previous step and produce a trajectory $T_{ij}^s = \{n_i^s, p_1^s, p_2^s, ..., n_j^s\}$.

Create occupancy map ($O(t)$): In this step, multiple pairs of nodes were generated as described in the previous step. These generated nodes were input to CTF to obtain a set of trajectories $\tau = \{T_1, T_2, ...,\}$. These are the set of trajectories used for quantifying the preferred pose of objects of interest as described in section 3.2. These trajectories were mapped to the floor in the geometry to create an occupancy map $O(t_i)$ which quantifies the number of times a trajectory passes through a triangle t_i as used in quantifying the amount of view of regions with dominant activity in section 3.2. A snapshot of the occupancy map from the simulated trajectories T in G is shown in Figure 5.

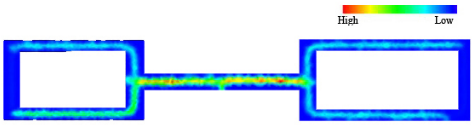

Figure 5: Occupancy map ($O(t)$) of the hallway obtained by mapping multiple simulated trajectories. Red indicating regions of dominant activity and blue with minor activity.

Clustering algorithm: The regions that belong to the same cluster should have a similar value of occupancy and also be located in the same spacial location. A point's spatial co-ordinates and it's occupancy $(c_i, O(t_i))$ were used as features, where $c_i = \{x_i, y_i, z_i\}$ are the 3D co-ordinates of the centroid of triangle t_i and $O(t_i)$ it's occupancy. The clusters obtained by using Expectation Maximization (EM) (Dempster et al., 1977) are shown in Figure 6. In this scenario, red

Table 1: Identified clusters and their mean occupancies.

No.	Cluster	Occupancy
1	Blue	0.23
2	Red	**0.42**
3	Green	0.13
4	Aqua	0.11
5	Light Pink	0
6	Pink	0.11

cluster was identified to have the highest average human occupancy followed by blue and then pink as shown in Table 1.

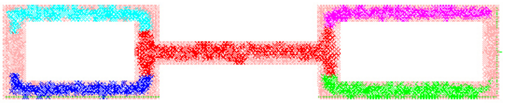

Figure 6: Clusters of regions with dominant activity in the geometry obtained by EM algorithm.

4.1.3 RRHC Optimization

Once the clusters are identified, the optimization is applied on each cluster separately. Given a cluster, first the points in the ceiling that have a view of the centroid of the cluster are identified and these points are considered as the possible location of the cameras. The only possible orientation for a camera are pointing towards the points on the floor in the cluster. This would simplify the problem to finding two points, one on the ceiling to position the camera and the second on the floor to point the camera towards. As described in section 3.3, random restart hill climbing optimization was performed to find the two optimal points.

4.2 Results

The motivation for this work was to optimize the camera placement in the geometry to provide effective surveillance as defined in section 1. A configuration of cameras in a geometry is considered to provide effective surveillance if it maximizes the below quantities while minimizing the number of cameras. Such a system is effective both in terms of surveillance and cost. Hence all the quantities used for comparison are normalized by the number of cameras in the configuration.

- **Area of observable space in view**: The total area accessible by humans in view of the camera is calculated for all the cameras and normalized.
- **Amount of activity in view**: To quantify the occupancy of a location that is in view, the activity produced in that location is considered. The number of frames that have motion in them are used as a metric to define the activity of the location that is viewed from the camera. The normalized value is used as a metric.
- **Pose of objects of interest and their resolution**: Assuming that a certain number of pixels are required for face detection. Face detection is used to quantify the pose of objects of interest along with their resolution. The number of faces detected are counted for every camera in the configuration and normalized.

The above metrics are defined to assess these qualities in a configuration of cameras. The configuration generated by the proposed method is compared to the following method.

- **3 coloring solution (Fisk, 1978):** A solution to Art Gallery Problem (AGP) was obtained using the 3 coloring solution and the cameras were placed at these locations. This configuration was used as baseline. The geometry of the environment's polygon contains holes. The polygon was modified to remove the holes and then 3 coloring solution was computed for the polygon. The cameras were manually placed to maximize the area in view. The solution is as shown in Figure 7.

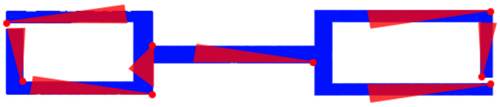

Figure 7: Configuration of cameras obtained by computing 3 coloring solution to AGP.

- **(Janoos et al., 2007)**: Janoos *et al.* defined cell coverage quality metric by taking observed human occupancy and resolution into account. This metric was used to optimize the camera location for each cluster. The following configuration was obtained, see Figure 8.

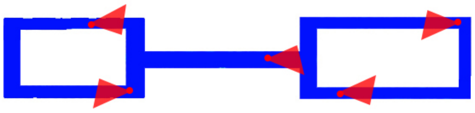

Figure 8: Configuration of cameras obtained by optimizing the cell coverage quality metric proposed bt Janoos *et al.* 2007 for each cluster.(Janoos et al., 2007)

- **(Huang et al., 2014)**: Huang *et al.* proposed a shortest watchman route solution and positioned wireless cameras along the route to maximize the view area of the polygon. Their solution was proposed only for simple polygons with out holes and hence the modified polygon was used in this case as well. The obtained configuration is shown in Figure 9.

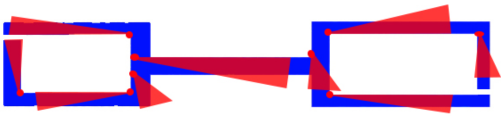

Figure 9: Configuration of cameras obtained by finding the shortest watchman route in the geometry as proposed by Huang *et al.* 2014(Huang et al., 2014).

- **Proposed method:** The obtained configuration from the proposed method is shown in Figure 10, and the view from the cameras are shown in Figure 11.

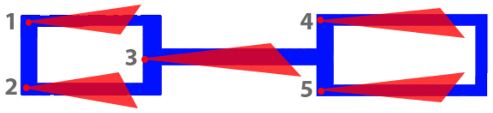

Figure 10: Configuration of cameras obtained from the proposed method.

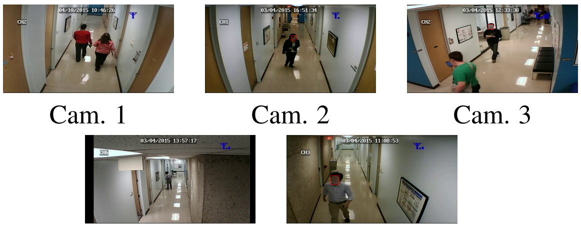

Cam. 1 Cam. 2 Cam. 3

Cam. 4 Cam. 5

Figure 11: Camera view from the cameras deployed in the test case scenario as calculated by the proposed method.

Table 2: Comparison of area and activity in view per camera.

Method	no. of cams.	Area/cam	Activity/cam
3 Coloring	8	0.057	28048.6
Janoos	5	0.01	44366.2
Huang	10	0.064	40092.5
Proposed	5	**0.109**	**69933.8**

Table 3: Faces counted from individual cameras in the proposed method.

Camera	Faces
Cam. 1	622
Cam. 2	3430
Cam. 3	**5929**
Cam. 4	915
Cam. 5	1930

Table 2 shows the area under view per camera. Although, 3 coloring solution and Huang *et al.* has higher area coverage, the number of cameras used is higher than that of the proposed method and the area in view per camera is higher for the proposed method.

All cameras used for experiments had a frame rate of 30fps. For each camera, the number of frames in which there is activity is counted using background subtraction. The average number of frames per camera are shown in Table 2. Most activity per camera was observed in the proposed method.

For each of these methods, a day's worth of data (10 hours) was collected. We have run face detection (Viola and Jones, 2001; Lienhart and Maydt, 2002) on these videos to count the number of faces captured. The number of faces captured for each camera are shown in Table 3. It can be noticed that Cam. 3 has the highest number of faces detected followed by Cam. 2. Cam. 3 is over-viewing the common hallway represented by the red cluster (see Table 1) with the highest simulated occupancy value. The average number of faces detected for each method are shown in Table 4. Approximately the same total number of faces were detected by 3 coloring solution and the proposed method, except for 3 coloring solution uses 8 cameras and the proposed method uses only 5 cameras. Using Huang et al. more than twice the total number of faces were detected than the proposed method but the number of cameras used were also twice as many than the proposed method. More than a quarter of the faces detected by Huang *et al.* configuration were from a single camera of the 10 cameras, which coincidentally happened to be focused at an elevator where people tend to stand and wait. The method proposed by Janoos *et al.* focuses on areas with high human occupancy and takes resolution of the triangle into account as opposed to the proposed method which uses the resolution of the approximate location of the face and hence their cameras are located above the regions of dominant human occupancy and fails to capture faces.

Although the proposed system performs better over the state of the art systems, some necessary im-

Table 4: Comparison of faces detected per camera.

Method	cameras	Faces/cam
3 Coloring	8	1264
Janoos	5	1111.8
Huang	10	2040.5
Proposed	5	**2183.6**

provements are to be taken into consideration. As noticed in Huang *et al.* configuration, significant number of faces were captured by focusing a camera at the elevator. This can be considered as a draw back of the proposed system and all the others being compared to, as none of the systems take the entrances and exits into consideration which could be valuable for surveillance. It would be interesting to incorporate a method to include the entrances and exits in the analysis. A method to estimate the number of cameras required for each cluster depending on the size of the cluster can be useful. If the cluster is big, it might be interesting to assign multiple cameras and incorporate a MCLP/BCLP problem formulation for optimization to ensure maximal coverage.

5 CONCLUSION

We have proposed an algorithm to optimize the placement of surveillance cameras in a 3D infrastructure by predicting the possible human behavior within the infrastructure. We have proposed a method to identify regions with dominant human activity. We have also proposed a metric that quantifies the position of a camera based on the observable space, activity in this space, pose of objects of interest within the activity and their image resolution in camera view for optimization. This method was compared with the state of the art algorithms and the obtained results show an improvement in the amount of area under view, observed activity and face detection rate per camera.

Acknowledgment

This work was supported in part by the US Department of Justice 2009-MU-MU-K004. Any opinions, findings, conclusions or recommendations expressed in this paper are those of the authors and do not necessarily reflect the views of our sponsors.

REFERENCES

Bodor, R., Drenner, A., Schrater, P., and Papanikolopoulos, N. (2007). Optimal camera placement for automated surveillance tasks. *Journal of Intelligent and Robotic Systems*, 50(3):257–295.

Chen, X. and Davis, J. (2000). Camera placement considering occlusion for robust motion capture. Technical report.

Debaque, B., Jedidi, R., and Prevost, D. (2009). Optimal video camera network deployment to support security monitoring. In *Information Fusion, 2009. FUSION '09. 12th International Conference on*, pages 1730–1736.

Dempster, A. P., Laird, N. M., and Rubin, D. B. (1977). Maximum likelihood from incomplete data via the em algorithm. *JOURNAL OF THE ROYAL STATISTICAL SOCIETY, SERIES B*, 39(1):1–38.

Erdem, U. M. and Sclaroff, S. (2004). Optimal placement of cameras in floorplans to satisfy task requirements and cost constraints. In *In Proc. of OMNIVIS Workshop*.

Filho, C., de Oliveira, A., and Costa, M. (2010). Using random restart hill climbing algorithm for minimization of component assembly time printed circuit boards. *Latin America Transactions, IEEE (Revista IEEE America Latina)*, 8(1):23–29.

Fisk, S. (1978). A short proof of Chvtal's Watchman Theorem. *Journal of Combinatorial Theory*, 24.

Fleishman, S., Cohen-Or, D., and Lischinski, D. (1999). Automatic camera placement for image-based modeling. In *Computer Graphics and Applications, 1999. Proceedings. Seventh Pacific Conference on*, pages 12–20, 315.

Hörster, E. and Lienhart, R. (2006a). Approximating optimal visual sensor placement. In *Multimedia and Expo, 2006 IEEE International Conference on*, pages 1257–1260.

Hörster, E. and Lienhart, R. (2006b). Calibrating and optimizing poses of visual sensors in distributed platforms. *Multimedia Systems*, 12(3):195–210.

Hörster, E. and Lienhart, R. (2006c). On the optimal placement of multiple visual sensors. In *Proceedings of the 4th ACM International Workshop on Video Surveillance and Sensor Networks*, VSSN '06, pages 111–120, New York, NY, USA. ACM.

Huang, H., Ni, C.-C., Ban, X., Gao, J., Schneider, A., and Lin, S. (2014). Connected wireless camera network deployment with visibility coverage. In *INFOCOM, 2014 Proceedings IEEE*.

Janoos, F., Machiraju, R., Parent, R., Davis, J. W., and Murray, A. (2007). Sensor configuration for coverage optimization for surveillance applications. In *SPIE, 2007 Proceedings*.

Kim, K. and Murray, A. T. (2008). Enhancing spatial representation in primary and secondary coverage location modeling*. *Journal of Regional Science*, 48(4):745–768.

Kitani, K., Ziebart, B., Bagnell, J., and Hebert, M. (2012). Activity forecasting. Lecture Notes in Computer Science, pages 201–214.

Lienhart, R. and Maydt, J. (2002). An extended set of haar-like features for rapid object detection. In *Image Processing. 2002. Proceedings. 2002 International Conference on*, volume 1, pages I–900–I–903 vol.1.

Malik, R. and Bajcsy, P. (2008). Automated Placement of Multiple Stereo Cameras. In *The 8th Workshop on Omnidirectional Vision, Camera Networks and Non-classical Cameras - OMNIVIS*, Marseille, France.

Rahul Swaminathan and Vincenzo Caglioti and Antonis Argyros.

Mantini, P. and Shah, S. (2014). Human trajectory forecasting in indoor environments using geometric context. In *Proceedings of the Ninth Indian Conference on Computer Vision, Graphics and Image Processing*, ICVGIP '14. ACM.

Mittal, A. and Davis, L. (2004). Visibility analysis and sensor planning in dynamic environments. In Pajdla, T. and Matas, J., editors, *Computer Vision - ECCV 2004*, volume 3021 of *Lecture Notes in Computer Science*, pages 175–189. Springer Berlin Heidelberg.

Murray, A. T., Kim, K., Davis, J. W., Machiraju, R., and Parent, R. (2007). Coverage optimization to support security monitoring. *Computers, Environment and Urban Systems*, 31(2):133 – 147.

Ram, S., Ramakrishnan, K. R., Atrey, P. K., Singh, V. K., and Kankanhalli, M. S. (2006). A design methodology for selection and placement of sensors in multimedia surveillance systems. In *Proceedings of the 4th ACM International Workshop on Video Surveillance and Sensor Networks*, VSSN '06, pages 121–130, New York, NY, USA. ACM.

Sivaram, G. S. V. S., Kankanhalli, M. S., and Ramakrishnan, K. R. (2009). Design of multimedia surveillance systems. *ACM Trans. Multimedia Comput. Commun. Appl.*, 5(3):23:1–23:25.

Tarabanis, K., Allen, P., and Tsai, R. (1995). A survey of sensor planning in computer vision. *Robotics and Automation, IEEE Transactions on*, 11(1):86–104.

Viola, P. and Jones, M. (2001). Rapid object detection using a boosted cascade of simple features. In *Computer Vision and Pattern Recognition, 2001. CVPR 2001. Proceedings of the 2001 IEEE Computer Society Conference on*, volume 1, pages I–511–I–518 vol.1.

Yabuta, K. and Kitazawa, H. (2008). Optimum camera placement considering camera specification for security monitoring. In *Circuits and Systems, 2008. ISCAS 2008. IEEE International Symposium on*, pages 2114–2117.

Zhang, Y., Lei, T., Barzilay, R., and Jaakkola, T. (2014). Greed is Good if Randomized: New Inference for Dependency Parsing. In *Proceedings of the 2014 Conference on Empirical Methods in Natural Language Processing (EMNLP)*. Association for Computational Linguistics.

Zhou, W., Xiong, H., Ge, Y., Yu, J., Ozdemir, H., and Lee, K. (2010). Direction clustering for characterizing movement patterns. In *Information Reuse and Integration (IRI), 2010 IEEE International Conference on*, pages 165–170.